

Cite this: *Chem. Sci.*, 2025, 16, 12012

All publication charges for this article have been paid for by the Royal Society of Chemistry

## Access to amidines via C(sp<sup>2</sup>)-N coupling of trifluoroborate-iminiums with *N*-fluorobenzenesulfonimide†

Damijan Knez, <sup>a</sup> Andrej Šterman, <sup>a</sup> Izidor Sosič, <sup>a</sup> Franc Perdih, <sup>b</sup> Gonzalo D. Nuñez, <sup>c</sup> Tilen Knaflič, <sup>de</sup> Denis Arčon, <sup>ef</sup> Maria Besora, <sup>c</sup> Jorge J. Carbó, <sup>c</sup> Elena Fernández <sup>c</sup> and Zdenko Časar <sup>g</sup>\*

Amidines are an important class of organic compounds with widespread application as superbases, nucleophilic catalysts, and building blocks of heterocyclic compounds in organic synthesis. Moreover, they represent an important structural motif in medicinal chemistry. This work describes an application of primary trifluoroborate-iminiums in unprecedented azide- and transition-metal-free transformation to *N*-sulfonyl amidines in the presence of *N*-fluorobenzenesulfonimide (NFSI). This novel C(sp<sup>2</sup>)-N bond-forming reaction proceeds without excess of any reagent, under mild conditions and provides good to high yields of *N*-sulfonyl amidines by a simple isolation procedure. Density functional theory (DFT) mechanistic studies into this novel transformation support that the use of a base is required to activate either the trifluoroborate-iminium or the NFSI and promote the C(sp<sup>2</sup>)-N bond formation via nucleophilic attack of the nitrogen. The utility of the developed methodology is showcased with the synthesis of two bioactive compounds.

Received 21st April 2025

Accepted 21st May 2025

DOI: 10.1039/d5sc02912k

rsc.li/chemical-science

## Introduction

Amidines<sup>1,2</sup> (Scheme 1A) are an important and ubiquitous group of compounds, which found versatile applications as key building blocks in heterocycle synthesis,<sup>3,4</sup> superbases in organic synthesis,<sup>5</sup> nucleophilic catalysts,<sup>6</sup> and are also common motifs in medicinal chemistry.<sup>7</sup> Several drugs contain the amidine moiety.<sup>8–11</sup> Unprotected amidines have traditionally been synthesized from nitriles, which are typically derived from

toxic cyanides,<sup>12</sup> using the Pinner reaction or other activation methods that necessitate the use of transition metals, cumbersome reagents, sulfur compounds, and harsh conditions. Alternatively, amides or thioamides are used with similar limitations (Scheme 1B).<sup>1</sup> Even modern synthetic approaches for amidine preparation continue to face these challenges.<sup>13</sup> Thus, the direct synthesis of protected amidines, followed by deprotection, could provide an alternative convenient approach to amidines. Among protected amidines, Boc-protected analogues are scarcely reported in the literature and face similar synthetic challenges related to sulfur chemistry.<sup>14</sup> In contrast, *N*-sulfonyl amidines are among the most extensively studied classes of protected amidines, which can be directly assembled. Interest in *N*-sulfonyl amidines (Scheme 1A), has gained momentum due to their biological properties.<sup>15</sup> Consequently, the preparation of *N*-sulfonyl amidines<sup>16,17</sup> and unsubstituted *N*-sulfonyl amidines<sup>18–24</sup> (Scheme 1A) has been extensively studied recently. Nevertheless, the syntheses of *N*-sulfonyl amidines and their unsubstituted counterparts are largely dependent on azide chemistry (Scheme 1C),<sup>16,17a–j,19–24</sup> which is hazardous even at laboratory scale.<sup>25</sup> This provides impetus for development of novel synthetic approaches to *N*-sulfonyl amidines. However, there is limited information available on the deprotection of *N*-sulfonyl amidines in the literature.<sup>23</sup> Interestingly, construction of C–N bonds as one of the most common structures in organic molecules, which is also found in amidines, is frequently dictated by transition-metal catalysis.<sup>26–32</sup> Accordingly, transition-metal-free

<sup>a</sup>University of Ljubljana, Faculty of Pharmacy, Aškerčeva cesta 7, 1000 Ljubljana, Slovenia. E-mail: zdenko.casar@ffa.uni-lj.si

<sup>b</sup>University of Ljubljana, Faculty of Chemistry and Chemical Technology, Večna pot 113, 1000 Ljubljana, Slovenia

<sup>c</sup>Departament de Química Física i Inorgànica, Universitat Rovira i Virgili, 43007 Tarragona, Spain

<sup>d</sup>Institute for the Protection of Cultural Heritage of Slovenia, Research Institute, Poljanska cesta 40, 1000 Ljubljana, Slovenia

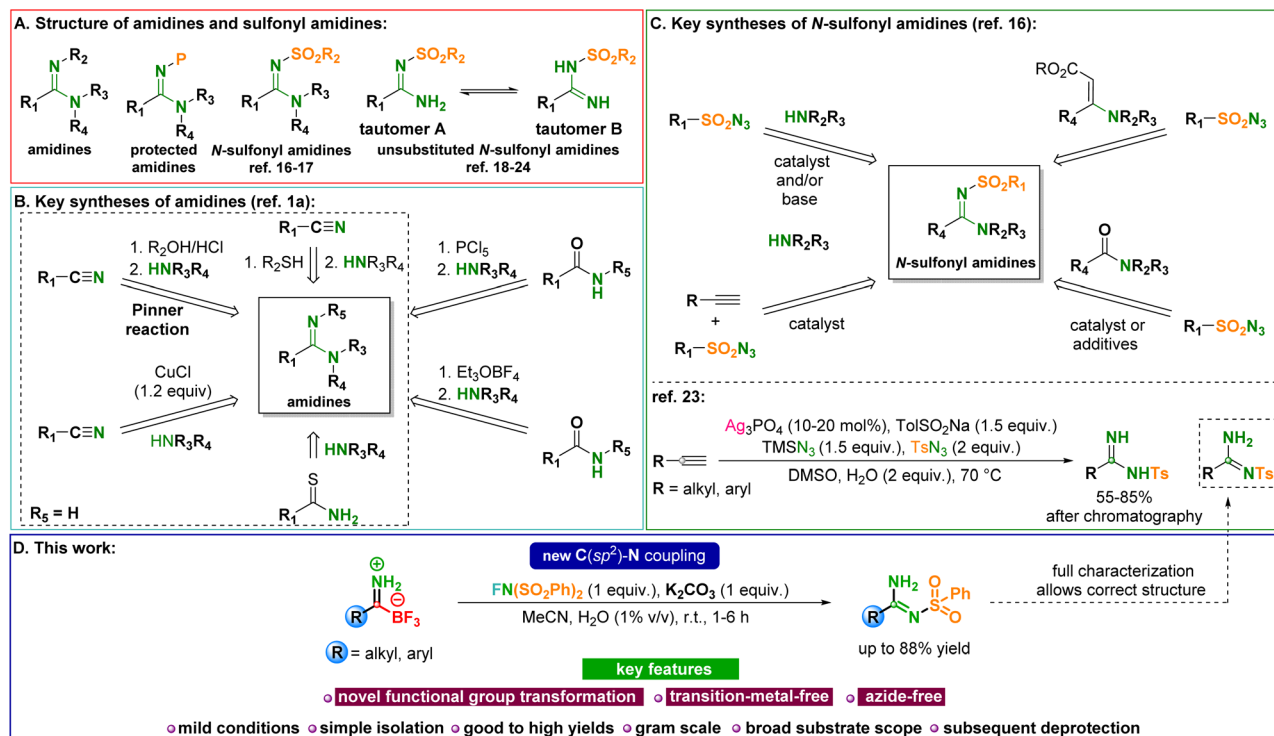
<sup>e</sup>Jožef Stefan Institute, Condensed Matter Physics Department, Jamova cesta 39, 1000 Ljubljana, Slovenia

<sup>f</sup>University of Ljubljana, Faculty of Mathematics and Physics, Jadranska 19, 1000 Ljubljana, Slovenia

<sup>g</sup>Lek Pharmaceuticals d.d., Sandoz Development Center Slovenia, Verovškova ulica 57, 1526 Ljubljana, Slovenia. E-mail: zdenko.casar@sandoz.com

† Electronic supplementary information (ESI) available: Experimental details, condition optimization tables, supplementary figures, product characterizations, spectral data for all new compounds, X-ray crystallographic data, and computational data (PDF). CCDC 2400597–2400604. For ESI and crystallographic data in CIF or other electronic format see DOI: <https://doi.org/10.1039/d5sc02912k>





Scheme 1 (A) Structure of amidines and sulfonyl amidines. (B) Key syntheses of amidines. (C) Key syntheses of *N*-sulfonyl amidines. (D) This work.

methodologies for the C–N bond formation remain a challenge and continue to be understudied.<sup>28,33</sup> The application of organoboron compounds as synthons in organic synthesis has enabled myriad of useful transformations,<sup>34–36</sup> including transition-metal-catalyzed C–N bond formation using Chan–Lam<sup>37</sup> and aminative Suzuki–Miyaura reaction.<sup>38</sup> Recently, we reported the first synthesis and transformation of primary trifluoroborate-iminiums (pTIMs).<sup>39</sup> The unique properties of pTIMs inspired us to further explore their late-stage functionalization with other reagents in order to extend their scope and utility. For this purpose, we explored the reaction of alkyl substituted pTIMs with *N*-fluorobenzenesulfonimide (NFSI),<sup>40</sup> a well-known fluorinating reagent that also participates in amination reactions catalyzed by different transition metals.<sup>41</sup> Surprisingly, instead of the anticipated  $\alpha$ -methylene fluorination, the C(sp<sup>2</sup>)–N bond-forming reaction took place yielding the *N*-sulfonyl amidine derivative despite the reaction being performed in the absence of transition metals. In this report, we present findings on this investigation and provide mechanistic insights into this novel C–N bond-forming transformation (Scheme 1D). To the best of our knowledge, this represents an unprecedented functional group transformation and azide- and transition-metal-free access to *N*-sulfonyl amidines. With this work we expand the scope of transition-metal-free C–N bond formation reactions.<sup>28,33</sup>

## Results and discussion

In the initial experiment, primary trifluoroborate-iminium (pTIM) **1a** reacted with NFSI (3 equiv.) in the presence of

K<sub>2</sub>CO<sub>3</sub> (2 equiv.) and molecular sieves (3 Å) in acetonitrile under strict water-free conditions, at ambient temperature (Table 1) as it was described by De Kimpe and coworkers for fluorination of imines.<sup>40</sup> After 0.5 h, almost no reaction was observed (Table 1, entry 1). Subsequent sampling of the reaction mixture after 1 h

Table 1 Reaction of pTIM **1a** with NFSI and its optimization

Entry <sup>a</sup>	NFSI (equiv.)	K <sub>2</sub> CO <sub>3</sub> (equiv.)	Additive	2a <sup>b</sup> [%]		
				0.5 h	1.0 h	3.0 h
1	3	2	MS 3 Å	4	18	46
2	3	2	MS 3 Å	nd	nd	26
3	3	2	10% H <sub>2</sub> O	99	100	100
4	3	2	1% H <sub>2</sub> O	95	100	100
5	1	1	10% H <sub>2</sub> O	93	100	100
6	1	1	1% H <sub>2</sub> O	47	83	100
7	1	0.1	1% H <sub>2</sub> O	20	26	29
8	1	0	1% H <sub>2</sub> O	0	0	0

<sup>a</sup> Reactions were conducted by using **1a** (0.2 mmol) at 0.1 M concentration. <sup>b</sup> The conversion into **2a** was determined by <sup>1</sup>H-NMR and was calculated as  $I_{2a}/(I_{1a} + I_{2a}) \times 100\%$ , where  $I_{1a}$  and  $I_{2a}$  are integrals for CH<sub>3</sub> of **1a** and **2a**, respectively (see ESI Fig. S1–S8). nd = not determined.



and 3 h showed that 18% and 46% of product **2a** was formed, respectively (Table 1, entry 1). Characterization of the product by NMR, HRMS and single crystal X-ray analysis later confirmed the unexpected formation of unsubstituted *N*-sulfonyl amidine **2a**. Performing the reaction in a strictly closed system without any interim sampling led to significantly lower amount of **2a** (26%) after 3 h (Table 1, entry 2). This result suggested that additional moisture introduced during the sampling in the initial experiment (Table 1, entry 1) may have promoted the reaction. To investigate this effect, we conducted the reaction without molecular sieves and with 10% (v/v) added water. Interestingly, 99% of **2a** was obtained after just 0.5 h (Table 1, entry 3), indicating that the presence of water was crucial for the reaction's success. Lowering the amount of added water to 1% (v/v) did not affect the reaction outcome (Table 1, entry 4). Using stoichiometric amounts of NFSI and K<sub>2</sub>CO<sub>3</sub> in the presence of 10% (v/v) water provided 93% of **2a** after 0.5 h, with full conversion achieved after 1 h (Table 1, entry 5), significantly improving the reaction's atom economy. When 1% (v/v) of water was used in combination with stoichiometric amount of used K<sub>2</sub>CO<sub>3</sub> and NFSI, to avoid potential imine hydrolysis<sup>39</sup> at longer reaction times, full conversion to **2a** was achieved in 3 h (Table 1, entry 6). In contrast, catalytic amount of the base (0.1 eq.) resulted in only 29% conversion to **2a** after 3 h (Table 1, entry 7). Moreover, in the absence of K<sub>2</sub>CO<sub>3</sub>, no reaction occurred (Table 1, entry 8). A similar trend was observed for pTIM with aryl substituent (Table S1 and Fig. S9†).

With the optimal reaction conditions in hand, we evaluated the scope of the transformation. Various aliphatic substituents including linear alkyl (**1a**), branched alkyl (**1b** and **1c**), hydroxylated alkyl (**1d**) and cyclic alkyl (**1e** and **1f**) were well tolerated, affording the desired unsubstituted *N*-sulfonyl amidines **2a–f** in good to high yields (62–85%, Scheme 2A) after simple isolation using solvent evaporation and extraction. Next, we evaluated a broad scope of pTIMs **1** containing electron-donating (EDG) or electron-withdrawing (EWG) groups on aromatic rings. pTIMs **1g–s** bearing mono- and disubstituted aryl rings, provided the corresponding products **2g–s** in good to high yields (65–88%, Scheme 2A) regardless of the nature of the substituent on the aromatic ring. Interestingly, substrates **1** containing EDG groups on aryl ring (**1h**, **1l**, **1m**, **1n**, and **1s**) provided products in slightly higher yields compared to their counterparts containing EWG groups (**1i–k** and **1o–r**). In addition, pTIMs **1t–v** featuring five-membered thiophene and furan rings smoothly underwent C–N bond formation to afford the corresponding unsubstituted *N*-sulfonyl amidines **2t–v** in 71–80% yield.

Noteworthy, as in the case of aliphatic substrates, pure products **2g–o** and **2r–v** were isolated by simple solvent evaporation and extraction, while for substrates **2p** and **2q** chromatographic isolation was required due to the low volatility of ethyl cyanobenzoate side products (*vide infra*).

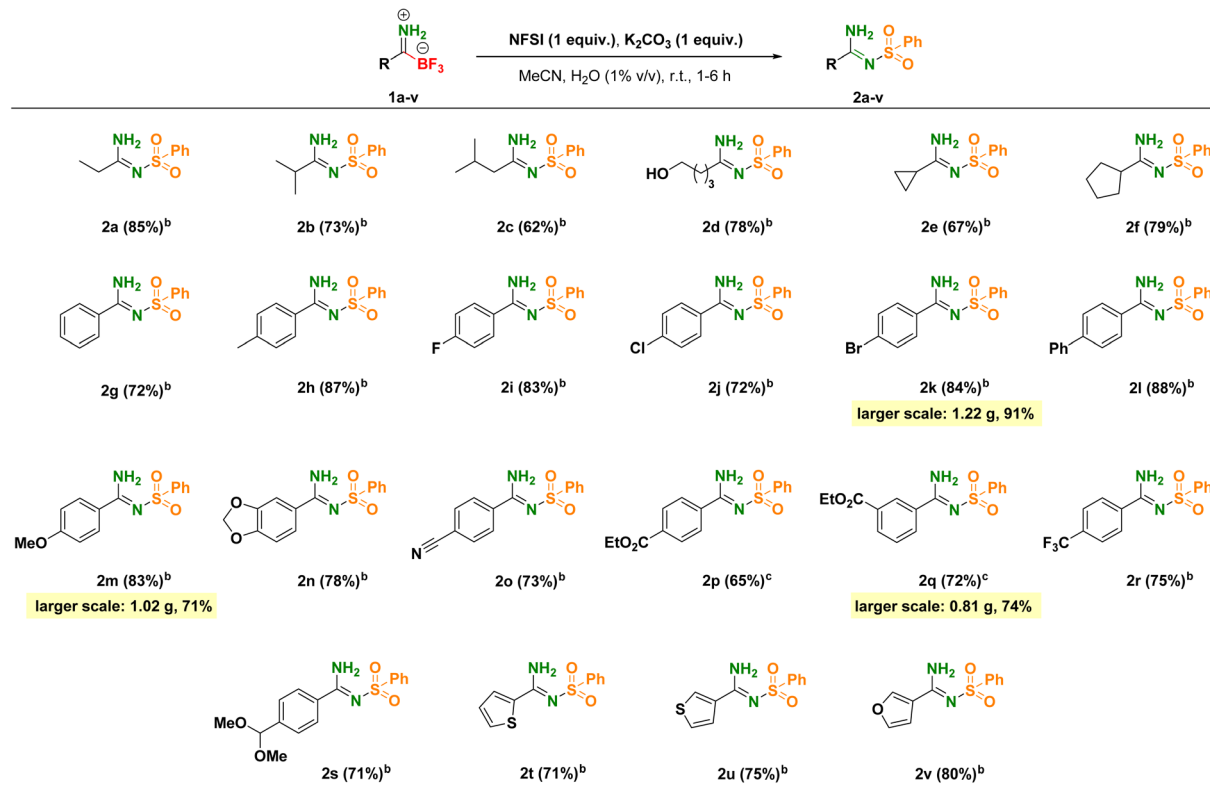
An interesting case in the reaction scope investigation was *meta*-phenol substrate **1w**, which provided a mixture of two products **2w** and **2w'**, in a 1 : 1.25 ratio with an overall yield of 69%. The formation of **2w'** can be explained by subsequent reaction of **2w** with benzenesulfonyl fluoride by-product, which is formed from NFSI (*vide infra*). Finally, pyridyl substrate **1x** led

to reactions with multiple side products, and in the best case, the desired **2x** was isolated in 41% yield after chromatographic purification (Scheme 2B).

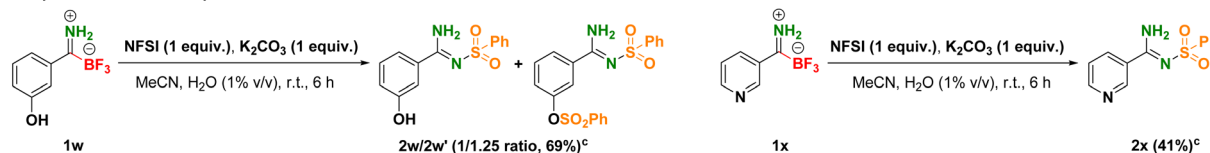
By applying the optimal reaction conditions established in the screening phase, the reaction was successfully scaled-up for substrates **1k**, **1m**, and **1q** giving the corresponding products **2k**, **2m**, and **2q** in 0.81–1.22 grams and 71–91% yield (Scheme 2A), which demonstrated the feasibility of the developed C–N bond-forming methodology.

Ambiguity exists in the literature regarding the structure of unsubstituted *N*-sulfonyl amidines, with some reports supporting tautomeric form **A**,<sup>15d,16,18–22,24</sup> while others propose tautomeric form **B**.<sup>16,23</sup> (Scheme 1A). To resolve this uncertainty, we focused on determining the structure of isolated products **2**. Initially, we conducted <sup>1</sup>H NMR, 2D <sup>1</sup>H–<sup>1</sup>H COSY NMR and 2D <sup>1</sup>H–<sup>15</sup>N HSQC NMR spectroscopy studies on compounds **2a**, **2f**, <sup>15</sup>N-**2f**, **2m** and <sup>15</sup>N-**2m** (Fig. S10–S31†). Examination of **2a** *via* NMR spectroscopy revealed that in the <sup>1</sup>H NMR spectrum (DMSO-*d*<sub>6</sub> at 400 MHz, 295 K) two broad signals of equal intensity appeared in the 7–9 ppm region at  $\delta_{\text{H}}$  8.53 ppm and  $\delta_{\text{H}}$  7.93 ppm, which were assigned to NH protons (Fig. S10†). Notably, at a higher temperature (DMSO-*d*<sub>6</sub> at 400 MHz, 353 K), a similar spectrum was observed with slightly broadened NH proton signals located at  $\delta_{\text{H}}$  8.31 and  $\delta_{\text{H}}$  7.79 ppm, which remained well separated (Fig. S11†). This indicates that **2a** exists as a single tautomeric form across a broad temperature range (295–353 K) in DMSO-*d*<sub>6</sub>. In MeCN-*d*<sub>3</sub> at 295 K, both NH signals were observed at  $\delta_{\text{H}}$  7.72 ppm and  $\delta_{\text{H}}$  6.90 ppm (Fig. S12†). Importantly, 2D <sup>1</sup>H–<sup>15</sup>N HSQC NMR spectrum in MeCN-*d*<sub>3</sub> revealed correlation signals between both NH protons located at  $\delta_{\text{H}}$  6.90 ppm and  $\delta_{\text{H}}$  7.72 ppm and a single nitrogen atom located at  $\delta_{\text{N}}$  106.8 ppm, confirming that both NH protons are attached to the same nitrogen atom (Fig. S13†). Similar results were observed for products **2f** and **2m**, as confirmed by their <sup>1</sup>H NMR and 2D <sup>1</sup>H–<sup>15</sup>N HSQC NMR spectra (Fig. S14–S21†). Furthermore, we synthesized <sup>15</sup>N-labeled compounds **2f** and **2m**, namely <sup>15</sup>N-**2f** and <sup>15</sup>N-**2m** using <sup>15</sup>N-pTIMs <sup>15</sup>N-**1f** and <sup>15</sup>N-**1m**. In the <sup>1</sup>H NMR spectrum (MeCN-*d*<sub>3</sub>) of <sup>15</sup>N-**2f**, we observed two sets of doublet of doublets signals for NH protons located at  $\delta_{\text{H}}$  6.92 ppm ( $J = 93.2$  and  $2.5$  Hz) and at  $\delta_{\text{H}}$  7.76 ppm ( $J = 91.3$  and  $2.5$  Hz) (Fig. S22†). The 2D <sup>1</sup>H–<sup>1</sup>H COSY NMR spectrum of <sup>15</sup>N-**2f** showed correlations between the NH signals at  $\delta_{\text{H}}$  6.82 ppm and  $\delta_{\text{H}}$  7.05 ppm, and another set of NH signals at  $\delta_{\text{H}}$  7.64 ppm and  $\delta_{\text{H}}$  7.87 ppm (Fig. 1A and S23†). In the <sup>1</sup>H–<sup>15</sup>N NMR coupled spectrum, the <sup>15</sup>N-labeled nitrogen in <sup>15</sup>N-**2f** appeared as a triplet signal at  $\delta_{\text{N}}$  106.9 ppm ( $J = 92.2$  Hz), which is characteristic for <sup>1</sup>H–<sup>15</sup>N couplings,<sup>42</sup> and in the <sup>1</sup>H–<sup>15</sup>N NMR decoupled spectrum as a singlet signal at nearly the same chemical shift (Fig. S24 and S25†). The 2D <sup>1</sup>H–<sup>15</sup>N HSQC NMR spectrum of <sup>15</sup>N-**2f** in MeCN-*d*<sub>3</sub> again confirmed correlation signals between the NH proton signals located at ( $\delta_{\text{H}}$  6.92 ppm and  $\delta_{\text{H}}$  7.74 ppm) and nitrogen atom at  $\delta_{\text{N}}$  107.0 ppm, verifying that both NH protons are attached to the labeled <sup>15</sup>N-nitrogen (Fig. 1B and S26†). The same set of NMR experiments conducted on aromatic derivative <sup>15</sup>N-**2m** yielded the same outcome (Fig. S27–S31†). These studies conclusively



A. Scope of pTIMs reaction with NFSI and larger scale synthesis of unprotected *N*-sulfonyl amidines:

## B. Special substrate examples:



Scheme 2 (A) Scope of primary trifluoroborate-iminiums reaction with NFSI<sup>a</sup> and larger scale synthesis of unprotected *N*-sulfonyl amidines. (B) Special substrate examples. <sup>a</sup>Reaction carried out with 0.20–0.80 mmol scale. Reaction times were: 1 h for 1a and 1c, 2 h for 1b, 1d and 1f and 6 h for all other substrates. Isolated yields are reported. <sup>b</sup>Isolation using solvent evaporation and extraction. <sup>c</sup>Isolation using column chromatography. See ESI† for details.

demonstrate that compounds 2 exist in solution as tautomeric structure A (Scheme 1A).

Moreover, during the reaction screening and scope investigation single crystals of 2a, 2e, 2h, 2j, 2m, 2p and 2u suitable for single crystal X-ray diffraction were obtained (Fig. 2A, S32–S41 and Table S2†). In all crystal structures, the N–C=N–S fragment is almost planar with dihedral angles ranging from 1.02 to 7.73°, with the exception of structure 2u where the dihedral angle is 13.49°. Such orientation enables the formation of intramolecular N–H⋯O hydrogen bonding between one hydrogen atom of the amino group and one oxygen atom of the sulfonyl group. The N⋯O distances in the range 2.702–2.886 Å indicate strong intramolecular hydrogen bonding (Table S3†). Additional hydrogen bonding interactions of the amino groups leads to different hydrogen-bonding motifs in the studied structures. In 2a three N–H⋯O interactions are present between the amino group and three sulfonyl groups. A bifurcated hydrogen bonding interaction enables the formation of hydrogen-bonded centrosymmetric dimers with the

aforementioned intramolecular hydrogen bonding as well as the intermolecular hydrogen bonding with the sulfonyl group of the adjacent molecules. Furthermore, the second hydrogen atom of the amino group interacts with adjacent sulfonyl group connecting these centrosymmetric dimers into centrosymmetric tetramers and thus the 1D belt is formed (Fig. S35†). In 2e, 2m and 2u intermolecular N–H⋯O interaction between the amino group and the sulfonyl group of the adjacent molecule enables the formation of hydrogen-bonded chain (Fig. S36, S39 and S41†). In 2h and 2j three crystallographically independent molecules are present in the asymmetric unit. In both structures each amino group is involved in three N–H⋯O interactions with three sulfonyl groups; a bifurcated hydrogen bonding interaction (intramolecular and intermolecular) and additional intermolecular hydrogen bonding with the sulfonyl group of the adjacent molecules. These interactions enable the formation of hydrogen-bonded belt in both structures (Fig. S37 and S38†). In 2p also three N–H⋯O interactions are present with the amino group as a hydrogen-bond donor. A bifurcated hydrogen



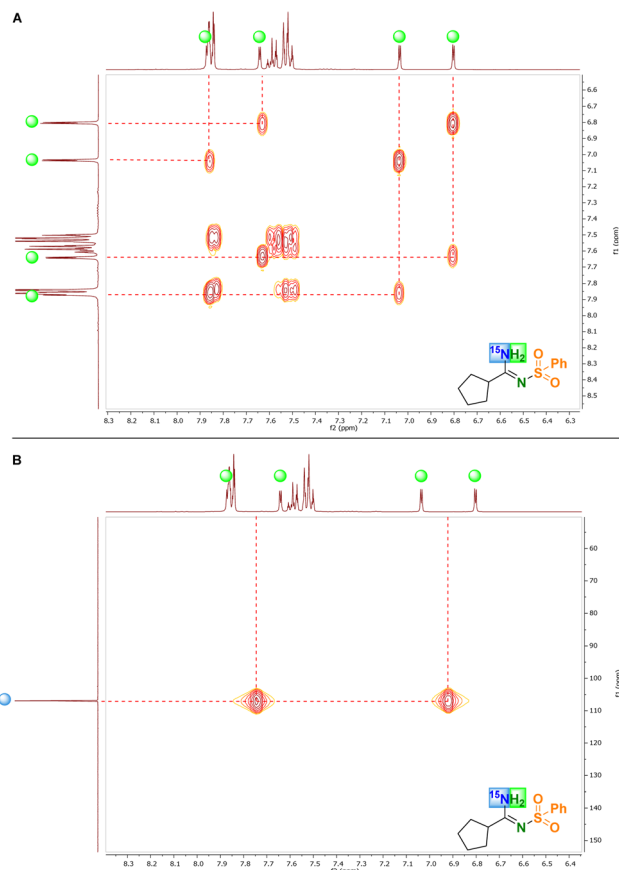


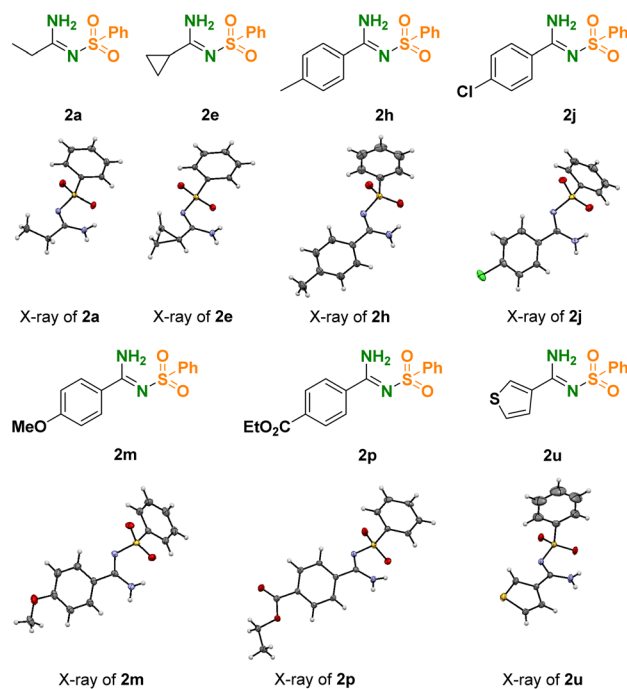
Fig. 1 (A)  $^1\text{H}$ - $^1\text{H}$  COSY NMR of  $^{15}\text{N}$ -2f in  $\text{MeCN-d}_3$  at 295 K and (B)  $^1\text{H}$ - $^{15}\text{N}$  HSQC NMR spectrum of  $^{15}\text{N}$ -2f in  $\text{MeCN-d}_3$  at 295 K.

bonding interaction is present with intramolecular hydrogen bonding as observed in all studied structures as well as intermolecular  $\text{N-H}\cdots\text{O}$  interactions between the amino group and the sulfonyl group of the adjacent molecule enabling the formation of hydrogen-bonded chain. The second hydrogen atom of the amino group connects these chains into layer through the interaction with the carbonyl oxygen atom of the adjacent molecule (Fig. S40 $^\dagger$ ). Therefore, the analysis of residual electron density maps (Fig. S32–S34 $^\dagger$ ) and the described hydrogen-bonding motifs (Fig. 2A and S35–S41 $^\dagger$ ) unequivocally support the tautomeric form A (Scheme 1A) for products 2 in the solid state.

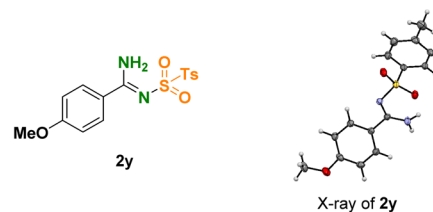
Interestingly, Bi *et al.*<sup>23</sup> made similar products using a silver-catalyzed four-component transformation of alkynes (Fig. 1C) and proposed tautomeric structure B for obtained products based on  $^1\text{H}$  NMR,  $^{13}\text{C}$  NMR spectra and the single crystal structure of one product. However, repetition of Bi's procedure provided product 2y (Fig. 2B), which showed tautomeric structure A in both solution and solid state as confirmed by  $^1\text{H}$  NMR, 2D  $^1\text{H}$ - $^{15}\text{N}$  HSQC NMR (Fig. S43–S46 $^\dagger$ ), and single crystal X-ray analysis (Tables S2, S3 and Fig. S42 $^\dagger$ ).

Therefore, both NMR spectroscopy and single crystal analysis clearly demonstrate that unsubstituted *N*-sulfonyl amidines 2 exist as tautomeric form A, both in solution and solid state.

#### A. Single crystal X-ray structure of the prepared products obtained in this work:



#### B. Single crystal X-ray structure of product 2y obtained using Bi's procedure:



#### C. DFT relative free-energies ( $\text{kcal mol}^{-1}$ ) of tautomeric forms of 2y:

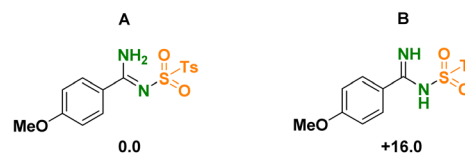


Fig. 2 (A) Single crystal X-ray structure of products 2a, 2e, 2h, 2j, 2m, 2p and 2u. (B) Single crystal X-ray structure of product 2y obtained using Bi's procedure.<sup>23</sup> (C) DFT relative free-energies in  $\text{kcal mol}^{-1}$  of two tautomeric forms of 2y (A and B).

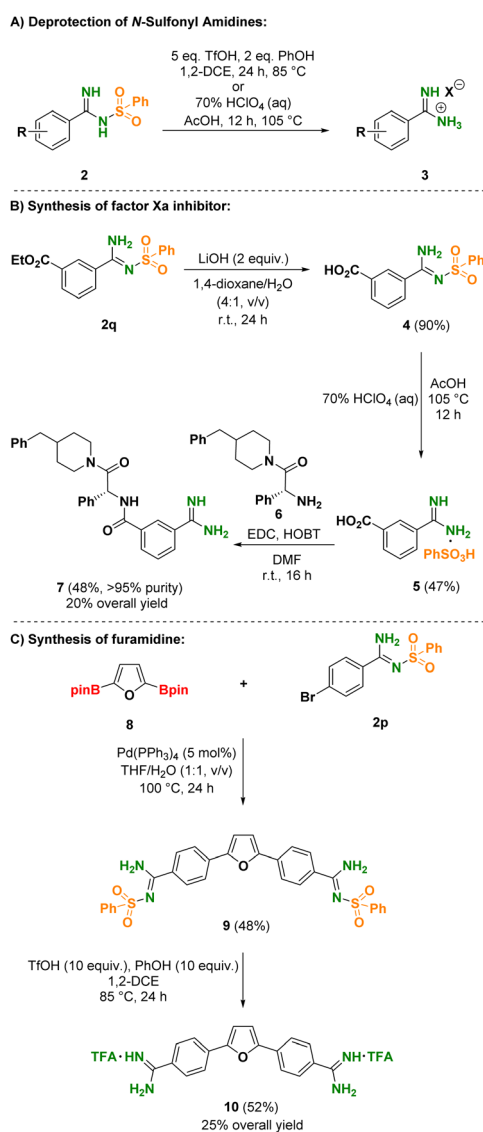
To rationalize the observed tautomeric structure A in products 2, we have performed DFT calculations (see below for details) to evaluate the relative free-energy of the tautomeric forms A and B in products 2 (Fig. 2C). In all the analysed cases, 2a, 2g, 2m and 2y, the tautomeric form A is significantly more stable than form B by 18.6, 16.0, 15.9 and 16.0  $\text{kcal mol}^{-1}$ , respectively, which agrees with experimental observations (see ESI $^\dagger$  for details).

Although sulfonyl amidines represent an interesting group of compounds on their own right,<sup>15</sup> we wanted to extend the utility and synthetic applications of the developed C–N bond-forming methodology to unsubstituted amidines. To that end, we first studied the removal of benzenesulfonyl group from the



unprotected *N*-sulfonyl amidines **2**. To our surprise, treatment of **2h** with NaOH in MeOH at reflux, as reported by Bi and co-workers,<sup>23</sup> did not provide the corresponding amidine **3**. We then studied approximately 30 different methodologies previously reported in the literature for deprotection of sulfonamides (see ESI† for details). Notably, only TfOH/phenol<sup>43–45</sup> or HClO<sub>4</sub> in AcOH<sup>46</sup> enable the sulfonyl group deprotection of unprotected *N*-sulfonyl amidines **2** to amidines **3** (Scheme 3A and ESI pages S54–S58†). Using the discovered synthetic approach and knowledge gained on the deprotection of sulfonyl amidines we prepared two bio active compounds: factor Xa inhibitor derivative **7**<sup>47</sup> and furamidine **10**,<sup>48</sup> in 20% and 25% overall yield in three and two steps, respectively, starting from **2q** and **2p** (Schemes 3B, C and ESI pages S59–S63†).

Finally, we wanted to shed light on the reaction mechanism. Important insights into the reaction mechanism were already obtained in the reaction screening experiments, which revealed



Scheme 3 Deprotection (A) and synthetic application of *N*-sulfonyl amidines in the synthesis of factor Xa inhibitor (B) and furamidine (C).

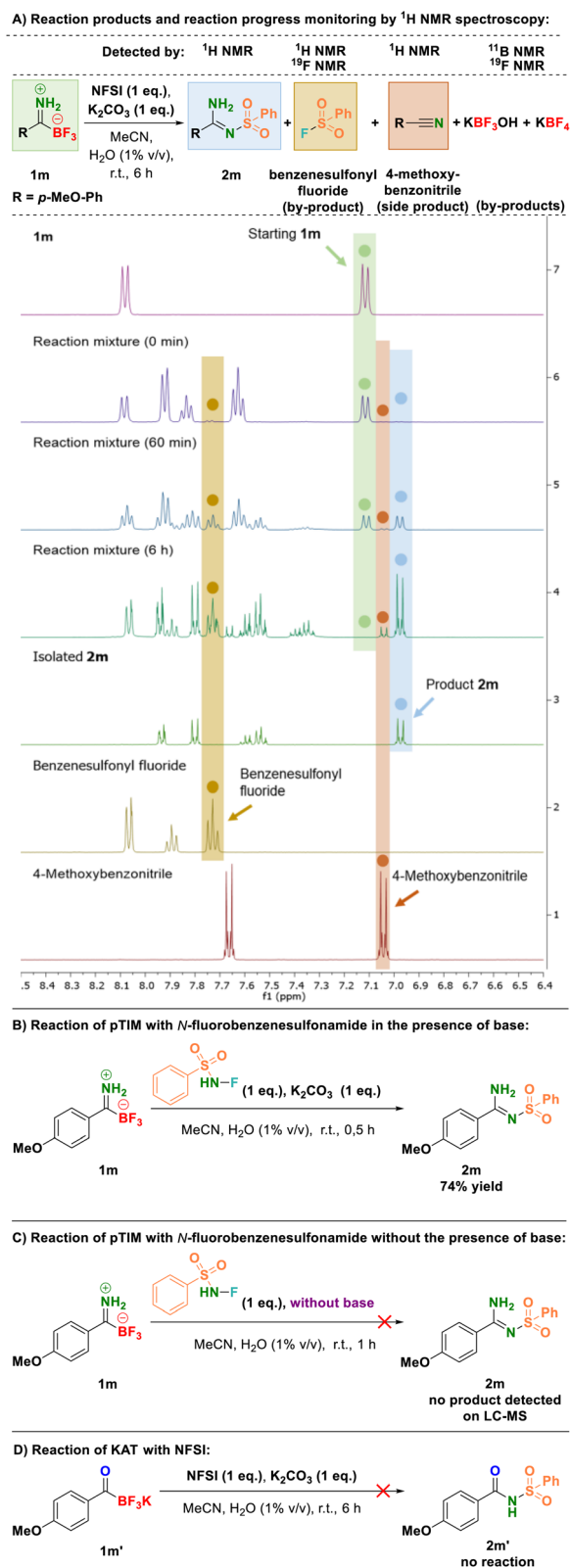
that the presence of K<sub>2</sub>CO<sub>3</sub> is mandatory for the reaction to proceed, and the water accelerates the reaction (Table 1). This suggests that the presence of the deprotonated form of pTIM **1a** may be essential for the reaction progress (Fig. S70†). Water likely plays an important role by solubilizing the inorganic base. To better understand the reaction, we monitored the conversion of **1a** to **2a** by <sup>1</sup>H-, <sup>11</sup>B- and <sup>19</sup>F-NMR (Fig. S71–S75†) in order to identify key species formed in the reaction mixture. These studies revealed that propionitrile (CH<sub>3</sub>CH<sub>2</sub>CN) as minor side product and benzenesulfonyl fluoride (PhSO<sub>2</sub>F) as a by-product were formed beside **2a**. In addition, we observed that two inorganic boron containing compounds were produced along the reaction: potassium hydroxytrifluoroborate (KBF<sub>3</sub>OH) as a major product and potassium tetrafluoroborate (KBF<sub>4</sub>) as a minor product (Fig. S48A and S59–S68†). We also monitored the reaction progress using <sup>1</sup>H NMR spectroscopy with substrate **1m** (Scheme 4A). Similarly, the formation of benzenesulfonyl fluoride and 4-methoxybenzotrile was confirmed by comparison with authentic reference compounds (Fig. S59, S60 and S69†).

For further insights, several control experiments were carried out (ESI pages S64–S102 and Fig. S48†). First, we examined if the reaction involves radical species, given that NFSI has a low N–F bond dissociation energy and is known to participate in many radical fluorination and amination transformations.<sup>41</sup> Experiments that excluded light and included radical scavengers were indicative of non-radical mechanism (Fig. S48C and S76–S80†). This was ultimately proved by direct reaction monitoring using continuous wave X-band EPR spectroscopy, which demonstrated that the reaction mixture was EPR silent (Fig. S48D and S81–S84†). The role of the observed nitrile side products as reaction intermediates was excluded by reaction of 4-methoxybenzotrile with dibenzenesulfonimide, benzenesulfonimide and NFSI (Fig. S48F and S86–S89†).

It is well-established that NFSI reacts with hard nucleophiles (*e.g.* nitrogen and oxygen nucleophiles) at sulfur. In the reaction of NFSI with hydroxide ions, benzenesulfonate anion and *N*-fluorobenzenesulfonamide (PhSO<sub>2</sub>NHF) are produced.<sup>49</sup> This prompted us to explore PhSO<sub>2</sub>NHF as a potential reaction intermediate in the conversion of **1m** to **2m**. We first prepared PhSO<sub>2</sub>NHF according to the procedure described by Qing and co-workers.<sup>50</sup> Subsequently, the reaction of **1m** with PhSO<sub>2</sub>NHF resulted in the formation of **2m**, which was isolated in 74% yield (Scheme 4B and Fig. S93, S94†). It is important to note that the reaction was completed in just 30 minutes, with no starting material observed in the <sup>1</sup>H NMR spectrum. This is significantly faster compared to the standard conditions using NFSI instead of *N*-fluorobenzenesulfonamide, where the reaction took over an hour (Fig. S95†). Interestingly, when **1m** was reacted with PhSO<sub>2</sub>NHF without the presence of K<sub>2</sub>CO<sub>3</sub>, no reaction took place as it was observed for reactions with NFSI (Scheme 4C and Fig. S96†). This additionally indicates that the deprotonation of pTIM **1m** and PhSO<sub>2</sub>NHF (pK<sub>a</sub> ≤ 0 was estimated for PhSO<sub>2</sub>NHF<sup>49</sup>) may be essential for the reaction to take place.

Moreover, these experiments suggest that deprotonated PhSO<sub>2</sub>NHF might likely be key intermediate species involved in the formation of products **2**.<sup>51,52</sup> Indeed, PhSO<sub>2</sub>NF<sup>–</sup> was





**Scheme 4** (A) Reaction products and reaction progress monitoring by  $^1\text{H}$  NMR. Key control experiments: reaction of pTIM **1m** with  $\text{PhSO}_2\text{-NH-F}$  in the presence of base (B) and absence of base (C); reaction of KAT **1m'** under standard conditions (D).

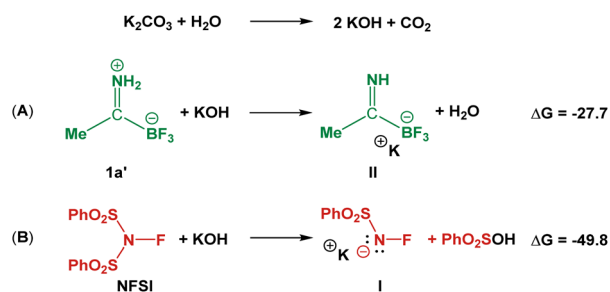
detected by LC-HRMS (ESI) analysis of the reaction mixture ( $[\text{M} - \text{H}]^-$ , found 174.0024, calculated 174.0031) together with benzenesulfonate ( $\text{PhSO}_3^-$ ;  $[\text{M} - \text{H}]^-$ , found 156.9958, calculated 156.9965) (Table S6 and Fig. S97 $\dagger$ ).

To verify the importance of imine structure in the substrate for the observed reactivity, potassium acyltrifluoroborates (KAT) **1m'** was subjected to the standard reaction conditions, which provided no reaction (Scheme 4D and Fig. S85 $\dagger$ ). This suggests that the imine structure in pTIMs **1** plays a crucial role in their coupling with NFSI and may be involved in the activation of NFSI *via* the formation of *N*-fluoroimine intermediates which are known to react readily with nitrogen nucleophiles.<sup>53</sup>

Bode's group recently demonstrated that C-to-N 1,2- $\text{BF}_3$  migrations, initially discovered by Yudin *et al.*<sup>54</sup> on B-MIDA acylboronates, represent a key step in amide formation during the ligation of KATs with hydroxylamines<sup>55,56</sup> and *N*-chloroamines.<sup>57</sup> Based on the apparent similarities to Bode's chemistry, the C-to-N 1,2- $\text{BF}_3$  migration process might be important for our mechanistic pathway, although the reaction initiation is apparently different.

To gain further insights into the reaction mechanism, we carried out DFT calculations ( $\omega\text{B97X-D/6-311g++(d,p)/SMD}$  level, for details see ESI pages S103–S117 $\dagger$ ). As a model substrate we selected the aliphatic pTIM **1a'** (Scheme 5), which is analogous to compound **1a** but replacing the ethyl by a methyl group to simplify the conformational complexity. Experimentally, we observed that the C( $\text{sp}^2$ )-N coupling of pTIM with NFSI requires stoichiometric amounts of base (see above). Thus, as computational model of the base, we used KOH molecule, which can be formed through the interaction of  $\text{K}_2\text{CO}_3$  with  $\text{H}_2\text{O}$  (see Scheme 5, top).

We can hypothesize that the reaction initiates with the base activation of one reactant, the other, or both. The deprotonation of pTIM (**1a'**) and desulfonation of NFSI are largely exergonic, irreversible processes with  $\Delta G = -27.7$  and  $-49.8$  kcal mol $^{-1}$ , respectively (Scheme 5A and B). Note that the free-energy differences are large enough to ignore the modeling limitations of strong bases in polar solvents. Importantly, the resulting species, the deprotonated form of pTIM (**II**) and  $\text{PhSO}_2\text{NF}^-$  (**I**), have been characterized by NMR and HRMS techniques in the reaction mixture of **1m** (Fig. S102 and S98, $\dagger$  respectively). The deprotonation of pTIM by KOH base to yield compound **II** proceeds downhill



**Scheme 5** Representation of the postulated initial acid–base reactions for deprotonation of pTIM **1a'** (A) and defluorination of NFSI (B). DFT free-energies kcal mol $^{-1}$ .



without barrier in the potential energy surface (Fig. S101†). Hence, the process would be controlled by the diffusion of reactants, for which we can assume a low free-energy barrier of approximately 3 kcal mol<sup>-1</sup> (Scheme 5A). Similarly, the free-energy scan of the desulfonylation by KOH base to give compound **I** and PhSO<sub>2</sub>OH indicates that the process occurs without significant energy barrier (Fig. S103†). Thus, both, compounds **II** and **I** can be formed under reaction conditions, but the modeling limitations of acid–base chemistry in solution do not allow estimating the ratio between **II** and **I**. From base activated species **II** and **I** depicted in Schemes 5A and B, we can envision two different reactive scenarios: reaction of species **II** with NFSI (mechanism A), and reaction of species **I** with **1a'** (mechanism B), both giving the corresponding *N*-sulfonyl amidine **2a'**.

Fig. 3A shows the computed free-energy profile for formation of sulfonyl amidine product **2a'** from **II** and NFSI following mechanism A. This mechanism is energetically feasible with a low overall free-energy barrier of 15.6 kcal mol<sup>-1</sup> (**II** + NFSI → **TS<sub>II-IV</sub>**). Moreover, this mechanism releases potassium hydroxytrifluoroborate KBF<sub>3</sub>OH as by-product, which was identified as the major boron product by <sup>11</sup>B NMR (in reaction with **1a**; Fig. S72†). The mechanism can be divided into 4 main steps (Fig. 3A): (i) the conjugated base of pTIM (species **II**) undergoes an electrophilic fluorination by the NFSI yielding intermediate **IV**; (ii) the defluorinated NFSI attacks nucleophilically the C(sp<sup>2</sup>) of intermediate **IV** forming the new C–N bond in the tetrahedral intermediate **V**, and subsequently, the K<sup>+</sup> counterion assists the concerted 1,2-shift of BF<sub>3</sub> and F substituents releasing intermediate **VI**; (iii) the fluoride substituent attacks intramolecularly the sulfonyl moiety in *syn* to yield the benzenesulfonyl fluoride (PhSO<sub>2</sub>F), which is detected by <sup>19</sup>F-NMR as by-product in the reaction of **1a** (see above and Fig. S73†), together with the borylated *N*-sulfonyl amidine **VII**; and (iv) final hydrolysis of BF<sub>3</sub> in **VII** gives the sulfonyl amidine product **2a'** and the potassium hydroxytrifluoroborate (KBF<sub>3</sub>OH), which is detected as a major product in the reaction of **1a** (see above and Fig. S72†). Interestingly, the analysis of HRMS spectra obtained upon injection of reaction mixture with reactant **1m** shows a peak whose mass (found 357.06956, calculated 357.06975) corresponds to a species analogous to intermediate **VII** (Table S7 and Fig. S100†) further supporting this mechanistic proposal. All the main steps of the mechanism are thermodynamically favorable with low energy barriers, being the electrophilic fluorination of intermediate **II** (**TS<sub>II-IV</sub>**) the most energy demanding step (see Fig. 3A). Note also that the conversion of intermediate **V** to **VI** proceeds with a very smooth energy barrier, suggesting that it can occur concertedly.

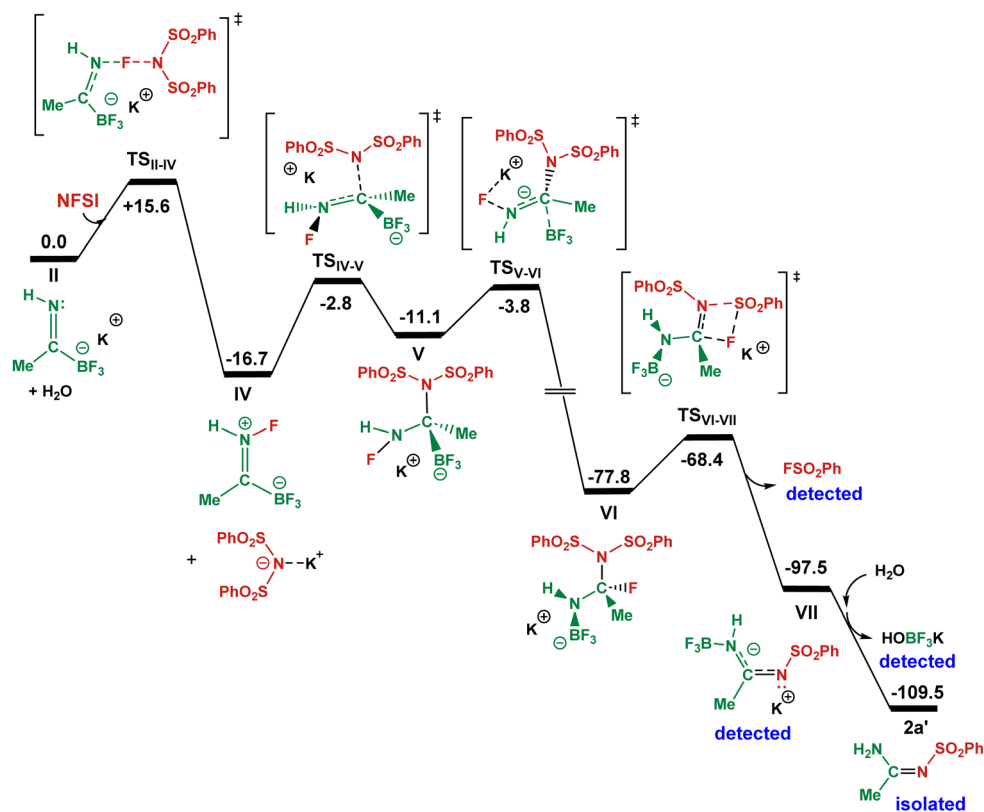
In the second reactive scenario, the species **I**, in which a highly nucleophilic nitrogen was generated, reacts with pTIM **1a'** to give **2a'** (mechanism B). Fig. 3B shows the computed free-energy profile for mechanism B, for which the overall free-energy barrier (9.8 kcal mol<sup>-1</sup>, **III** → **TS<sub>III-VIII</sub>**) is also low. This mechanism can be divided into 3 major reaction steps (Fig. 3B): (i) the desulfonylated NFSI, PhSO<sub>2</sub>NF<sup>-</sup> (**I**), attacks nucleophilically reactant **1a'** forming the new N–C bond with a very low free-energy barrier (2.2 kcal mol<sup>-1</sup>), (ii) the resulting intermediate **III**, which was detected by HRMS (ESI) analysis of the reaction mixture (in reaction with **1m**; [M]<sup>-</sup>, found

377.0755, calculated 377.0760, Fig. S99†), undergoes the electrophilic defluorination by K<sup>+</sup> cation with the concomitant release of KF and the C to N 1,2-shift of BF<sub>3</sub> group to intermediate **VIII**, and (iii) the deborylation in **VIII** by KF releases the final product **2a'** and the by-product KBF<sub>4</sub> that was confirmed as a boron product by <sup>11</sup>B NMR (in reaction with **1a**; Fig. S72†). The potassium tetrafluoroborate (KBF<sub>4</sub>) was observed as a minor boron product what may indicate that mechanism B operates in a minor extent. However, KBF<sub>4</sub> can react with the excess of KOH (2 equiv.) to form the potassium hydroxytrifluoroborate (KBF<sub>3</sub>OH) observed as a major boron product and whose process is exergonic by 24.7 kcal mol<sup>-1</sup> according to DFT calculations (see Fig. S106†). We also note that the ionized form of intermediate **VIII** could correspond to the HRMS spectral peak for the reaction mixture of **1m** (Table S7 and Fig. S100†). In contrast to mechanism A, in mechanism B, the 1,2-BF<sub>3</sub> migration is not accompanied by the reverse 1,2-F migration. This was confirmed by IRC calculations at the corresponding transition state **TS<sub>III-VIII</sub>** (see Fig. 3B) followed by geometry optimization.

The overall computational results are consistent with previous computational studies in related reactions and with experimental observations. Bode and co-workers<sup>56</sup> have computationally studied a related process: the C(sp<sup>2</sup>)-N formation in amide ligations by reaction of potassium acyltrifluoroborates (KAT) and *O*-substituted hydroxyl amines.<sup>56</sup> This current mechanistic proposal shares some chemical features with Bode's work such as the C–N bond formation through the nucleophilic attack of the N-containing reactant (**TS<sub>IV-V</sub>** and **TS<sub>I-III</sub>**) to yield a tetrahedral intermediate (**V** and **III**), or the nitrogen-heteroatom bond cleavage with concomitant 1,2-BF<sub>3</sub> migration (**TS<sub>V-VI</sub>** and **TS<sub>III-VIII</sub>**). Moreover, our calculations indicate that the C(sp<sup>2</sup>)-N cross-coupling of trifluoroborate-iminium with NFSI proceeds through two simultaneous pathways, the one (mechanism A) starts from conjugated base of the iminium, and the other one (mechanism B) starts from the base-activated NFSI species PhSO<sub>2</sub>NF<sup>-</sup> (**I**). With these reactive scenarios, it is possible to explain the formation of all the intermediates and by-products observed experimentally in reaction of **1a** or **1m**: the active forms of the reactants **I** and **II** (Scheme 5), the boron by-products KBF<sub>3</sub>OH and KBF<sub>4</sub>, the by-product PhSO<sub>2</sub>F, and the reaction intermediates **III**, **VII**, and **VIII**. Interestingly, in both mechanisms A and B the rate-determining steps involve an electrophilic process: the electrophilic fluorination of species **II** in mechanism A (**TS<sub>II-IV</sub>**) and the K<sup>+</sup> cation abstraction of the fluoride of intermediate **III** in mechanism B (**TS<sub>III-VIII</sub>**). This explains why the addition of electron donating groups in the aryl substituent of pTIM results in slightly higher yields (see above). The proposed mechanisms are also consistent with the observed stereoselectivity of product **2**, in which the amino and sulfonyl substituents of the C=N bond are in *cis* (Fig. S107†). In the stereo-determining step for mechanism A (**VI** → **VII**), the free-energy barrier conducting to **2a'** is 2.2 kcal mol<sup>-1</sup> lower than that for the opposite isomer, and the resulting intermediate **VII**, which could be reversely formed, is 2.7 kcal mol<sup>-1</sup>. For mechanism B, the difference in the irreversible stereo-selectivity determining step (**III** → **VIII**) is even larger (6.6 kcal mol<sup>-1</sup>) in favor of the observed isomer.



## A) Mechanism A:



## B) Mechanism B:

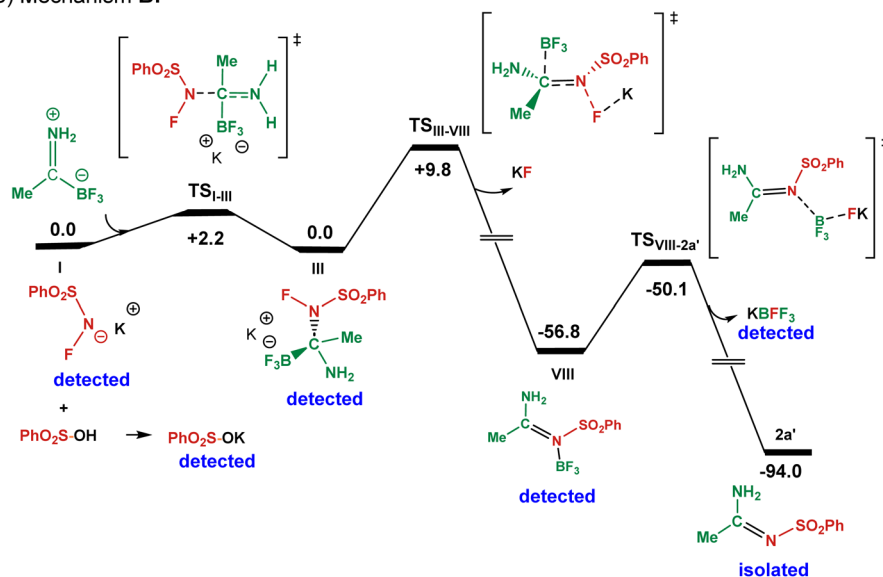


Fig. 3 Proposed mechanisms for the formation of unsubstituted *N*-sulfonyl amidines from pTIMs **1** and NFSI. Free-energy (kcal mol<sup>-1</sup>) profiles for the mechanism A with the zero-energy set at species II (A), and for the mechanism B with the zero-energy set at species I (B). Word "detected" indicates species detected experimentally during the reaction mechanism investigation on substrates **1a** or **1m**.

## Conclusions

In summary, we report a novel C–N bond-forming reaction featuring pTIMs and NFSI, which enables facile access to unsubstituted *N*-sulfonyl amidines. This unexpected C(sp<sup>2</sup>)-N coupling applies easily from accessible starting materials and

proceeds smoothly without excess of any reagents and under mild conditions. A broad range of aliphatic and aromatic pTIMs underwent the C(sp<sup>2</sup>)-N bond-forming reaction with NFSI in the presence of K<sub>2</sub>CO<sub>3</sub> and water giving a diverse range of unsubstituted *N*-sulfonyl amidines in good to high yields. DFT calculations showed that reaction is initiated by the base



activation of either the pTIMs or the NFSI reactant, yielding two distinct mechanisms that operate simultaneously. One of them starts by deprotonation of pTIM, whose conjugate base defluorinates NFSI increasing the nucleophilic character of its nitrogen and favoring C–N bond-forming. In the other reaction mechanism, the base desulfonylates NFSI generating a highly nucleophilic nitrogen able to attack the C(sp<sup>2</sup>) of pTIM to form the new C–N bond. In both mechanisms, the electrophilic defluorination of the nitrogen moiety by a potassium cation involves a concomitant C to N 1,2-BF<sub>3</sub> migration. The usefulness of the presented method was also demonstrated with the synthesis of factor Xa inhibitor derivative and furamidine. Thus, the methodology is especially suitable for the preparation of small *N*-sulfonyl amidine building blocks that can be incorporated into larger structures. The presented methodology opens new avenues in transition metal free C(sp<sup>2</sup>)-N coupling chemistry, as well as safe and sustainable new approach to functionalized amidines as important organic functionality.

## Data availability

The crystallographic data for structures reported in this study for compounds **2a**, **2e**, **2h**, **2j**, **2m**, **2p**, **2u** and **2y** have been deposited at the Cambridge Crystallographic Data Centre (CCDC), under accession numbers 2400597 (for **2a**), 2400598 (for **2e**), 2400599 (for **2h**), 2400600 (for **2j**), 2400601 (for **2m**), 2400602 (for **2p**), 2400603 (for **2u**) and 2400604 (for **2y**). These data can be obtained free of charge from The Cambridge Crystallographic Data Centre via [https://www.ccdc.cam.ac.uk/data\\_request/cif](https://www.ccdc.cam.ac.uk/data_request/cif).

## Author contributions

A. Š., I. S. and Z. Č. conceived the study. D. K., A. Š. and I. S. performed synthetic experiments and collected the data. I. S. and Z. Č. guided the synthesis research. Z. Č. wrote the introduction and synthetic part of the manuscript. F. P. performed the single crystal X-ray diffraction studies and wrote the corresponding discussion. T. K. and D. A. performed the EPR measurements, collected the data and wrote the corresponding discussion. E. F. co-guided the mechanistic study investigation. G. D. N., M. B. and J. J. C. performed the DFT calculations, collected the data and wrote the corresponding discussion. D. K., F. P., J. J. C. and E. F. performed editing of the manuscript. All authors discussed the results and contributed to the finalization of the paper. All authors have given approval to the final version of the manuscript.

## Conflicts of interest

There are no conflicts to declare.

## Acknowledgements

This work was supported by the Slovenian Research and Innovation Agency (research programmes P1-0208, P1-0230, P1-0125, and PhD grant to A. Š.). We also thank grant PID2021-

128128NB-I00 and PID2022-141693NB-I00 funded by MINECO/AEI/10.13039/501100011033 and by “ERDF A way of making Europe” and the Generalitat de Catalunya (2021SGR00110). Authors acknowledge Mrs M. Frelih and Dr S. Pajk for HRMS analyses. Authors thank Prof. Dr S. Stavber, Dr M. Črnugelj and Dr A. Meden for valuable discussions.

## Notes and references

- (a) P. J. Dunn, in *Comprehensive Organic Functional Group Transformations II*, ed. A. R. Katritzky and R. J. K. Taylor, Elsevier Science, Amsterdam, 2005, ch. 5.19, vol. 5, pp. 655–699; (b) R. L. Shriner and F. W. Neumann, *Chem. Rev.*, 1944, **35**(3), 351–425.
- T. Ishikawa and T. Kumamoto, in *Superbases for Organic Synthesis: Guanidines, Amidines, Phosphazenes and Related Organocatalysts*, ed. T. Ishikawa, John Wiley & Sons, Ltd, Chichester, 2009, ch. 3, pp. 49–91.
- F. Doraghi, S. Karimian, H. Navid, M. Ghanbarlou, B. Larijani and M. Mahdavi, *Monatsh. Chem.*, 2024, **155**, 419–439.
- (a) W. Guo, M. Zhao, W. Tan, L. Zheng, K. Tao and X. Fan, *Org. Chem. Front.*, 2019, **6**, 2120–2141; (b) Y. Zuo, P. Zuo, M. Liu, X. Wang, J. Du, X. Li, P. Zhang and Z. Xu, *Org. Biomol. Chem.*, 2024, **22**, 5014–5031.
- T. Ishikawa, *Superbases for Organic Synthesis: Guanidines, Amidines and Phosphazenes and Related Organocatalysts*, John Wiley & Sons, Ltd, Chichester, 2009.
- J. E. Taylor, S. D. Bull and J. M. J. Williams, *Chem. Soc. Rev.*, 2012, **41**(6), 2109–2121.
- (a) J. V. Greenhill and P. Lue, *Prog. Med. Chem.*, 1993, **30**, 203–326; (b) A. Z. Abidin, M. N. F. Norrahim, N. N. S. M. Shakrin, B. Ibrahim, N. Abdullah, J. I. A. Rashid, N. A. M. Kasim and N. A. A. Shah, *Heliyon*, 2024, **10**, e32010; (c) C. E. Rodrigues-Santos, M. R. de Brito and A. Echevarria, *J. Braz. Chem. Soc.*, 2024, **35**, e20240053.
- A. Porcheddu, G. Giacomelli and L. De Luca, *Curr. Med. Chem.*, 2012, **19**, 5819–5836.
- G. D. Diana, *J. Med. Chem.*, 1973, **16**, 857–859.
- L. A. Sorbera, J. Bozzo and J. Castañer, *Drugs Future*, 2005, **30**, 877–885.
- L. A. Sorbera, M. Bayès, J. Castañer and J. Silvestre, *Drugs Future*, 2001, **26**, 1155.
- (a) L. Vanoye, A. Hammoud, H. Gérard, A. Barnes, R. Philippe, P. Fongarland, C. de Bellefon and A. Favre-Réguillon, *ACS Catal.*, 2019, **9**, 9705–9714; (b) A. Hinzmann, T. Betke, Y. Asano and H. Gröger, *Chem.–Eur. J.*, 2021, **27**, 5313–5321; (c) M. Hinzmann, H. Yavuzer, M. Bittmann and H. Gröger, *Chem Catal.*, 2023, **2**, 100572.
- (a) D. A. Kissounko, J. M. Hoerter, I. A. Guzei, Q. Cui, S. H. Gellman and S. S. Stahl, *J. Am. Chem. Soc.*, 2007, **129**, 1776–1783; (b) A. Okano, R. C. James, J. G. Pierce, J. Xie and D. L. Boger, *J. Am. Chem. Soc.*, 2012, **134**, 8790–8793; (c) B. L. Korbad and S.-H. Lee, *Bull. Korean Chem. Soc.*, 2013, **34**, 1266–1268; (d) J. Sävmarker, J. Rydfjord, J. Gising, L. R. Odell and M. Larhed, *Org. Lett.*, 2012, **14**, 2394–2397; (e) M. M. Khalifa, M. J. Bodner, J. A. Berglund and



- M. M. Haley, *Tetrahedron Lett.*, 2015, **56**, 4109–4111; (f) I. I. Sahay, P. S. Ghalsasi, M. Singh and R. Begum, *Synth. Commun.*, 2017, **47**, 1400–1408; (g) Z. Zhang, B. Huang, G. Qiao, L. Zhu, F. Xiao, F. Chen, B. Fu and Z. Zhang, *Angew. Chem., Int. Ed.*, 2017, **56**, 4320–4323; (h) Z. Zhu, J. Cen, X. Tang, J. Li, W. Wu and H. Jiang, *Adv. Synth. Catal.*, 2018, **360**, 2020–2031; (i) K. M. van Vliet, L. H. Polak, M. A. Siegler, J. I. van der Vlugt, C. F. Guerra and B. de Bruin, *J. Am. Chem. Soc.*, 2019, **141**, 15240–15249; (j) Z.-Y. Gu, H. Han, Z.-Y. Li, S.-J. Ji and J.-B. Xia, *Org. Chem. Front.*, 2021, **8**, 1544–1550; (k) Y.-H. Fan, X.-Y. Guan, W.-P. Li, C.-Z. Lin, D.-X. Bing, M.-Z. Sun, G. Cheng, J. Cao, J.-J. Chen and Q.-H. Deng, *Org. Chem. Front.*, 2022, **9**, 380–385; (l) E. A. O'Brien, K. K. Sharma, J. Byerly-Duke, L. A. Camacho III and B. VanVeller, *J. Am. Chem. Soc.*, 2022, **144**, 22397–22402.
- 14 (a) C. L. Kusturin, L. S. Liebeskind and W. L. Neumann, *Org. Lett.*, 2002, **4**, 983–985; (b) E. De Vita, P. Schüler, S. Lovell, J. Lohbeck, S. Kullmann, E. Rabinovich, A. Sananes, B. Heßling, V. Hamon, N. Papo, J. Hess, E. W. Tate, N. Gunkel and A. K. Miller, *J. Med. Chem.*, 2018, **61**, 8859–8874; (c) P. P. Rashid, D. Singh and G. J. Sanjayan, *Tetrahedron Lett.*, 2019, **60**, 151254.
- 15 (a) L. Anglada, M. Marquez, A. Sacristan and J. Ortiz, *Eur. J. Med. Chem.*, 1988, **23**, 97–100; (b) H. D. Langtry, S. M. Grant and K. L. Goa, *Drugs*, 1989, **38**, 551–590; (c) S. S. Patel and M. I. Wilde, *Drugs*, 1996, **51**, 974–980; (d) K. Gobis, H. Foks, J. Sławiński, A. Sikorski, D. Trzybiński, E. Augustynowicz-Kopec, A. Napiórkowska and K. Bojanowski, *Monatsh. Chem.*, 2013, **144**, 647–658; (e) M.-J. Wang, Y.-Q. Liu, L.-C. Chang, C.-Y. Wang, Y.-L. Zhao, X.-B. Zhao, K. Qian, X. Nan, L. Yang, X.-M. Yang, H.-Y. Hung, J.-S. Yang, D.-H. Kuo, M. Goto, S. L. Morris-Natschke, S.-L. Pan, C.-M. Teng, S.-C. Kuo, T.-S. Wu, Y.-C. Wu and K.-H. Lee, *J. Med. Chem.*, 2014, **57**, 6008–6018; (f) Z.-L. Song, H.-L. Chen, Y.-H. Wang, M. Goto, W.-J. Gao, P.-L. Cheng, S. L. Morris-Natschke, Y.-Q. Liu, G.-X. Zhu, M.-J. Wang and K.-H. Lee, *Bioorg. Med. Chem. Lett.*, 2015, **25**, 2690–2693; (g) T. Beryozkina, V. Bakulev, L. Dianova, V. Berseneva, P. Slepukhin, J. Leban, P. Kalaba, N. Y. Aher, M. Ilic, H. H. Sitte and G. Lubec, *Synthesis*, 2016, **48**, 1046–1054; (h) T. Iwakawa, H. Tamura, M. Masuko, A. Murabayashi and Y. Hayase, *J. Pestic. Sci.*, 1992, **17**, 131–135; (i) M. S. A. El-Gaby, G. A. M. El-Hag Ali, A. A. El-Maghraby, M. T. Abd El-Rahman and M. H. M. Helal, *Eur. J. Med. Chem.*, 2009, **44**, 4148–4152; (j) M. Y. Lee, M. H. Kim, J. Kim, S. H. Kim, B. T. Kim, I. H. Jeong, S. Chang, S. H. Kim and S.-Y. Chang, *Bioorg. Med. Chem. Lett.*, 2010, **20**, 541–545; (k) L. Yang, Y.-L. Zhao, C.-Y. Zhao, H.-H. Li, M.-J. Wang, S. L. Morris-Natschke, K. Qian, K.-H. Lee and Y.-Q. Liu, *Med. Chem. Res.*, 2014, **23**, 5043–5057; (l) T. D. Suja, K. V. L. Divya, L. V. Naik, A. R. Kumar and A. Kamal, *Bioorg. Med. Chem. Lett.*, 2016, **26**, 2072–2076; (m) X. Nan, J. Zhang, H.-J. Li, R. Wu, S.-B. Fang, Z.-Z. Zhang and Y.-C. Wu, *Eur. J. Med. Chem.*, 2020, **200**, 112470.
- 16 Z. Xixi, L. Yunyun and W. Jie-Ping, *Chin. J. Org. Chem.*, 2020, **40**, 1891–1900.
- 17 (a) L. M. Fleury, E. E. Wilson, M. Vogt, T. J. Fan, A. G. Oliver and B. L. Ashfeld, *Angew. Chem., Int. Ed.*, 2013, **52**, 11589–11593; (b) A. Rouzi, R. Hudabaiardi and A. Wusiman, *Tetrahedron*, 2018, **74**, 2475–2481; (c) X. Zheng and J. P. Wan, *Adv. Synth. Catal.*, 2019, **361**, 5690–5694; (d) V. Ilkin, V. Berseneva, T. Beryozkina, T. Glukhareva, L. Dianova, W. Dehaen, E. Seliverstova and V. Bakulev, *Beilstein J. Org. Chem.*, 2020, **16**, 2937–2947; (e) C. G. Wang, R. Wu, T. P. Li, T. Jia, Y. Li, D. Fang, X. Chen, Y. Gao, H. L. Ni, P. Hu, B. Q. Wang and P. Cao, *Org. Lett.*, 2020, **22**, 3234–3238; (f) B. Kaboudin, S. Torabi, F. Kazemi and H. Aoyamab, *RSC Adv.*, 2020, **10**, 26701–26708; (g) Y. He and X. Wang, *Org. Lett.*, 2021, **23**, 225–230; (h) A. R. Liu, L. Zhang, J. Li and A. Wusiman, *RSC Adv.*, 2021, **11**, 15161–15166; (i) D. Yang, J. Shi, J. Chen, X. Jia, C. Shi, L. Ma and Z. Li, *RSC Adv.*, 2021, **11**, 18966–18973; (j) Z. Alassad, A. AboRaed, M. S. Mizrachi, M. H. Pérez-Temprano and A. Milo, *J. Am. Chem. Soc.*, 2022, **144**, 20672–20679; (k) K. A. DeKorver, W. L. Johnson, Y. Zhang, R. P. Hsung, H. Dai, J. Deng, A. G. Lohse and Y.-S. Zhang, *J. Org. Chem.*, 2011, **76**, 5092–5103; (l) Y. Kong, L. Yu, Y. Cui and J. Cao, *Synthesis*, 2014, **46**, 183–188; (m) Y. Feng, W. Zhou, G. Sun, P. Liao, X. Bi and X. Li, *Synthesis*, 2017, **49**, 1371–1379; (n) Q. Gou, Z. Liu, T. Cao, X. Tan, W. Shi, M. Ran, F. Cheng and J. Qin, *J. Org. Chem.*, 2020, **85**, 2092–2102; (o) B. Huang, C. Yang, J. Zhou and W. Xia, *Chem. Commun.*, 2020, **56**, 5010–5013; (p) D. Mishra, A. J. Borah, P. Phukan, D. Hazarika and P. Phukan, *Chem. Commun.*, 2020, **56**, 8408–8411; (q) F. Li, Z. Wu, J. Wang, S. Zhang, J. Yu, Z. Yuan, J. Liu, R. Shen, Y. Zhou and L. Liu, *Org. Chem. Front.*, 2022, **9**, 627–632; (r) C. S. Nishad, K. K. Haldar and B. Banerjee, *J. Org. Chem.*, 2022, **87**, 11644–11655; (s) Y.-C. Chou, W.-H. Lin, X.-Y. Lin, C.-L. Kuo, W.-Q. Zeng, I.-C. Lu and C.-F. Liang, *J. Org. Chem.*, 2022, **87**, 15327–15332; (t) Z. Zhang, X.-J. Meng, F.-H. Cui, H.-T. Tang, Y.-C. Wang, G.-B. Huang and Y.-M. Pan, *Org. Lett.*, 2024, **26**, 193–197; (u) C.-C. Cui, F. Lin, L.-Y. Wang, Y.-P. Liu, S.-J. Tu, M.-S. Tu, W.-J. Hao and B. Jiang, *Chem. Commun.*, 2024, **60**, 1492–1495; (v) J. Tian, M. Chen, X. Wang, X. Chen, C. Shao, Y. Xiong, Y. Liu and D. Sang, *Org. Biomol. Chem.*, 2024, **22**, 8663–8668; (w) J. K. Vankar, S. Tothadi and G. N. Gururaja, *Eur. J. Org. Chem.*, 2024, **27**, e202400776; (x) Q. Chevrier, T. Pierru, A. Craquelin, P. Maitrejean, A. Jean and L. Bettoni, *J. Org. Chem.*, 2024, **89**, 15282–15288.
- 18 K. Gobis, H. Foks, K. Wiśniewska, M. Dąbrowska-Szponar, E. Augustynowicz-Kopec, A. Napiórkowska and A. Sikorski, *Monatsh. Chem.*, 2012, **143**, 1161–1169.
- 19 J. Kim, S. Y. Lee, J. Lee, Y. Do and S. Chang, *J. Org. Chem.*, 2008, **73**, 9454–9457.
- 20 V. O. Filimonov, L. N. Dianova, K. A. Galata, T. V. Beryozkina, M. S. Novikov, V. S. Berseneva, O. S. Eltsov, A. T. Lebedev, P. A. Slepukhin and V. A. Bakulev, *J. Org. Chem.*, 2017, **82**, 4056–4071.



- 21 F. Yi, Q. Sun, J. Sun, C. Fu and W. Yi, *J. Org. Chem.*, 2019, **84**, 6780–6787.
- 22 V. O. Filimonov, L. N. Dianova, T. V. Beryozkina, D. Mazur, N. A. Beliaev, N. N. Volkova, V. G. Ilkin, W. Dehaen, A. T. Lebedev and V. A. Bakulev, *J. Org. Chem.*, 2019, **84**, 13430–13446.
- 23 B. Liu, Y. Ning, M. Virelli, G. Zanoni, E. A. Anderson and X. Bi, *J. Am. Chem. Soc.*, 2019, **141**, 1593–1598.
- 24 Y. Zhao, L. Li, Z. Zhou, M. Chen, W. Yang and H. Luo, *Org. Biomol. Chem.*, 2021, **19**, 3868–3872.
- 25 (a) T. Keicher and S. Löbbecke, in *Organic Azides: Syntheses and Applications*, ed. S. Bräse and K. Banert, John Wiley & Sons, Ltd, Chichester, 2010, ch. 1, pp. 1–27; (b) S. P. Green, K. M. Wheelhouse, A. D. Payne, J. P. Hallett, P. W. Miller and J. A. Bull, *Org. Process Res. Dev.*, 2020, **24**, 67–84.
- 26 J. F. Hartwig, *Acc. Chem. Res.*, 2008, **41**, 1534–1544.
- 27 D. Surry and S. Buchwald, *Angew. Chem., Int. Ed.*, 2008, **47**, 6338–6361.
- 28 J. Bariwalab and E. Van der Eycken, *Chem. Soc. Rev.*, 2013, **42**, 9283–9303.
- 29 J. Luo and W.-T. Wei, *Adv. Synth. Catal.*, 2018, **360**, 2076–2086.
- 30 I. P. Beletskaya and A. D. Averin, *Russ. Chem. Rev.*, 2021, **90**, 1359–1396.
- 31 R.-N. Zheng, H. Zheng, T. Li and W.-T. Wei, *ChemSusChem*, 2021, **14**, 5340–5358.
- 32 M. Rivas, V. Palchykov, X. Jia and V. Gevorgyan, *Nat. Rev. Chem.*, 2022, **6**, 544–561.
- 33 S. Roscales and A. G. Csáky, *Chem. Soc. Rev.*, 2020, **49**, 5159–5177.
- 34 D. G. Hall, *Boronic Acids: Preparation and Applications in Organic Synthesis, Medicine and Materials*, Wiley-VCH Verlag GmbH & Co. KGaA, Weinheim, 2011, vol. 1 and 2.
- 35 E. Fernández and A. Whiting, *Synthesis and Application of Organoboron Compounds*, Springer Cham, Heidelberg 2015.
- 36 E. Hey-Hawkins and C. Viñas Teixidor, *Boron-Based Compounds: Potential and Emerging Applications in Medicine*, John Wiley & Sons Ltd, Chichester, 2018.
- 37 (a) J. X. Qiao and P. Y. S. Lam, *Synthesis*, 2011, **2011**, 829–856; (b) M. J. West, J. W. B. Fyfe, J. C. Vantourout and A. J. B. Watson, *Chem. Rev.*, 2019, **119**, 12491–12523; (c) J.-Q. Chen, J.-H. Li and Z.-B. Dong, *Adv. Synth. Catal.*, 2020, **362**, 3311–3331.
- 38 P. Onnuch, K. Ramagonolla and R. Y. Liu, *Science*, 2024, **383**, 1019–1024.
- 39 A. Šterman, I. Sosič and Z. Časar, *Chem. Sci.*, 2022, **13**, 2946–2953.
- 40 G. Verniest, E. Van Hende, R. Surmont and N. De Kimpe, *Org. Lett.*, 2006, **8**, 4767–4770.
- 41 (a) G. Wang and J.-A. Ma, in *Fluorination. Synthetic Organofluorine Chemistry*, ed. J. Hu and T. Umemoto, Springer, Singapore, 2020, pp. 429–445; (b) Y. Li and Q. Zhang, *Synthesis*, 2015, **47**, 159–174; (c) Sushmita, T. Aggarwal, S. Kumar and A. K. Verma, *Org. Biomol. Chem.*, 2020, **18**, 7056–7073; (d) Q. Gu and E. Vessally, *RSC Adv.*, 2020, **10**, 16756–16768.
- 42 (a) S. L. Deev, I. A. Khalymbadzha, T. S. Shestakova, V. N. Charushin and O. N. Chupakhin, *RSC Adv.*, 2019, **9**, 26856–26879; (b) K. Singh and L. Frydman, *J. Phys. Chem. Lett.*, 2024, **15**, 5659–5664.
- 43 T. Javorskis and E. Orentas, *J. Org. Chem.*, 2017, **82**, 13423–13439.
- 44 B. E. Haskell and S. B. Bowlus, *J. Org. Chem.*, 1976, **41**, 159–160.
- 45 R. C. Roemmele and H. Rapoport, *J. Org. Chem.*, 1988, **53**, 2367–2371.
- 46 D. P. Kudav, S. P. Samant and B. D. Hosangadi, *Synth. Commun.*, 1987, **17**, 1185–1187.
- 47 S. D. Jones, J. W. Liebeschuetz, P. J. Morgan, C. W. Murray, A. D. Rimmer, J. M. E. Roscoe, B. Waszkowycz, P. M. Welsh, W. A. Wylie, S. C. Young, H. Martin, J. Mahler, L. Brady and K. Wilkinson, *Bioorg. Med. Chem. Lett.*, 2001, **11**, 733–736.
- 48 J. R. Jenquin, L. A. Coonrod, Q. A. Silverglate, N. A. Pellitier, M. A. Hale, G. Xia, M. Nakamori and J. A. Berglund, *ACS Chem. Biol.*, 2018, **13**, 2708–2718.
- 49 J. M. Antelo, J. Crugeiras, J. R. Leisa and A. Ríosa, *J. Chem. Soc., Perkin Trans. 2*, 2000, 2071–2076.
- 50 Y.-Y. Zhang, X.-H. Xu and F.-L. Qing, *Chin. J. Chem.*, 2022, **40**, 2956–2962.
- 51 B. D. Dond and S. N. Thore, *Tetrahedron Lett.*, 2020, **61**, 151660.
- 52 B. D. Dond, D. N. Pansare, A. P. Sarkate and S. N. Thore, *Chem. Pap.*, 2023, **77**, 1765–1772.
- 53 A. V. Fokin, A. T. Uzun and V. P. Stolyarov, *Russ. Chem. Rev.*, 1977, **46**, 1057–1072.
- 54 (a) Z. He and A. K. Yudin, *J. Am. Chem. Soc.*, 2011, **133**, 13770–13773; (b) Z. He, A. Zajdlík, J. D. St. Denis, N. Assem and A. K. Yudin, *J. Am. Chem. Soc.*, 2012, **134**, 9926–9929; (c) C. F. Lee, D. B. Diaz, A. Holownia, S. J. Kaldas, S. K. Liew, G. E. Garrett, T. Dudding and A. K. Yudin, *Nat. Chem.*, 2018, **10**, 1062–1070.
- 55 (a) A. M. Dumas, G. A. Molander and J. W. Bode, *Angew. Chem., Int. Ed.*, 2012, **51**, 5683–5686; (b) H. Noda and J. W. Bode, *Chem. Sci.*, 2014, **5**, 4328–4332.
- 56 M. Tanriver, Y.-C. Dzung, S. Da Ros, E. Lam and J. W. Bode, *J. Am. Chem. Soc.*, 2021, **143**, 17557–17565.
- 57 A. Osuna Gálvez, C. P. Schaack, H. Noda and J. W. Bode, *J. Am. Chem. Soc.*, 2017, **139**, 1826–1829.

